

Pressure-Induced Orientation Control of the Growth of Epitaxial Silicon Nanowires

A. Lugstein,^{*,†} M. Steinmair,[†] Y. J. Hyun,[†] G. Hauer,[†] P. Pongratz,[‡] and E. Bertagnolli[†]

Institute for Solid State Electronics, Vienna University of Technology, Floragasse 7, A-1040 Vienna, Austria, and Institute for Solid State Physics, Vienna University of Technology, Wiedner Hauptstr. 8/052, A-1040 Vienna, Austria

Received April 17, 2008

ABSTRACT

Single crystal silicon nanowires (SiNWs) were synthesized with silane reactant using Au nanocluster-catalyzed one-dimensional growth. We have shown that under our experimental conditions, SiNWs grown epitaxially on Si(111) via the vapor–liquid–solid growth mechanism change their growth direction as a function of the total pressure. Structural characterization of a large number of samples shows that SiNWs synthesized at a total pressure of 3 mbar grow preferentially in the $\langle 111 \rangle$ direction, while the one at 15 mbar favors the $\langle 112 \rangle$ direction. Specifically by dynamically changing the system pressure during the growth process morphological changes of the NW growth directions along their length have been demonstrated.

During the past decade significant progress has been made in the realization of appropriate 1D nanostructures, such as carbon nanotubes, NWs, and nanofibers.^{1–7} In particular, semiconductor NWs are natural candidates for a wide range of novel devices having applications in optoelectronics, nanoelectronics, and sensors.^{8–17} In developing these applications, it is important to control the electrical and optical properties of NWs, which strongly depend on the diameter¹⁸ as well as the crystallographic orientation¹⁹ and defect structure of the NWs.²⁰ Synthesis techniques using chemical vapor deposition (CVD),²¹ metalorganic CVD,²² molecular-beam epitaxy (MBE),^{23–25} and laser ablation techniques,²⁶ have therefore been directed at producing single crystal NWs with uniform diameters and controlled growth directions. The particular type we focus on here is the most rational and tunable vapor–liquid–solid (VLS) growth mechanism,^{21,27,28} superior for the fabrication of nanometer-sized wires. In the VLS growth of SiNWs, a metal such as Au is used as a catalyst agent to nucleate whisker growth from a Si-containing vapor. Au and Si form a liquid alloy that has a eutectic temperature of 364 °C, which upon supersaturation, nucleates the growth of a SiNW. For VLS growth, the NW diameter plays a crucial role in the growth direction.^{29,30} SiNWs of diameter greater than 40 nm prefer the $\langle 111 \rangle$ direction,³¹ whereas wires with less than 20 nm are mostly

$\langle 110 \rangle$ oriented.^{32,33} In the intermediate range also the $\langle 112 \rangle$ orientation is present.^{28,31,34,35} By applying the conventional epitaxial crystal growth technique into the VLS process, it is possible to achieve orientation control during the NWs growth. Having in mind the diameter dependency of the NW growth direction, one strategy to obtain highly ordered NWs is to suitably select the substrate and to control the metal particle size and reaction conditions so that the NWs grow epitaxially on the substrate. Yang and co-workers have achieved well-aligned SiNWs arrays by VLS epitaxy.³⁶ By controlling size, density, location, and growth direction of NWs, the methods shall enable their efficient and economical incorporation into devices. Furthermore, manipulation of the wire growth by changing the growth conditions during NW synthesis may provide a useful tool for increasing the range of structures that can be formed using the VLS technique. In this letter, we report on experiments demonstrating that the growth direction of epitaxially grown SiNWs changes with total growth pressure from $\langle 111 \rangle$ to $\langle 112 \rangle$ direction. To the best of our knowledge the influence of the pressure on the growth rate³⁷ and the morphology³⁸ is to some extent investigated but up to now a pressure dependency of the growth direction has not been discussed elsewhere.

The SiNWs were synthesized in a hot wall CVD reactor by the VLS growth mechanism using diluted silane (SiH₄) as precursor gas. Prior to the deposition of the catalyst, the native oxide on the Si(111) substrates was removed with a buffered hydrofluoric acid etch to create a hydrogen-

* Corresponding author. E-mail: alois.lugstein@tuwien.ac.at.

[†] Institute for Solid State Electronics, Vienna University of Technology.

[‡] Institute for Solid State Physics, Vienna University of Technology.

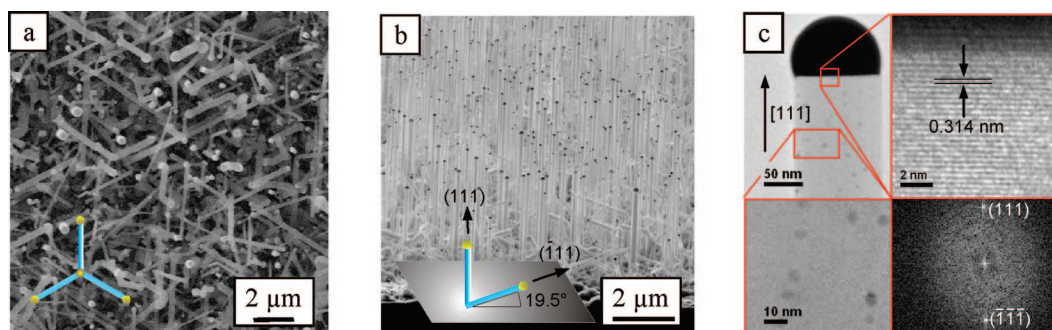


Figure 1. (a) Plan-view SEM image of SiNWs grown at 500 °C for 100 min on Si(111) at a total pressure of 3 mbar. (Inset: schematic top-view of $\langle 111 \rangle$ oriented NWs grown on a (111) substrate.) (b) Tilted view showing the slightly tapered NWs with solidified Au particles on top grown along $\langle 111 \rangle$ directions. (Inset: schematic side-view of $\langle 111 \rangle$ oriented NWs grown on a (111) substrate.) (c) TEM image of a single crystalline SiNW showing the catalytic Au nanoparticle cap and Au–Si particles about 7 nm in size on the sidewalls of the NWs. The HRTEM micrograph of the crystalline core shows clearly the Si(111) atomic planes, and the Fourier transform of the image proves the $[111]$ growth direction.

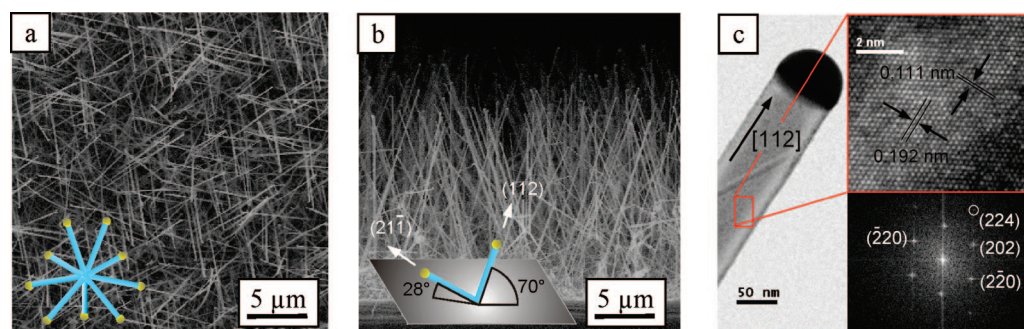


Figure 2. (a) Top-view SEM image of SiNWs grown at 500 °C for 60 min on Si(111) at a total pressure of 15 mbar. (Inset: schematic top-view of $\langle 112 \rangle$ oriented NWs grown on a (111) substrate.) (b) The cross-sectional view shows most of the rodlike NWs forming an angle of about 70° with respect to the Si(111) substrate independent of their diameter. (Inset: schematic side-view of $\langle 112 \rangle$ oriented NWs grown on a (111) substrate.) (c) TEM image of a 80 nm diameter SiNW with the less common $[112]$ growth direction. The insets show the HRTEM micrograph giving a closer view on the area marked with the red rectangle in the TEM image with the (224) atomic planes of the SiNW separated by 0.111 nm and the respective FFT diffraction pattern.

terminated surface. Gold served as a catalyst, which was deposited at room temperature as a film of 2 nm thickness via thermal evaporation. The growth was done at total pressures of 3 and 15 mbar using a 100 sccm flow of SiH_4 (2% in a He mixture) and 10 sccm hydrogen at a growth temperature of 500 °C. The growth was stopped by switching off the precursor gas, and the samples were cooled down in vacuum. The SiNWs were characterized by scanning electron microscopy (SEM) (ZEISS-LEO 1450) and high resolution transmission electron microscopy (HRTEM) (FEI TECNAI G20).

Figure 1a shows a typical top view SEM image, and Figure 1b shows the respective tilted view image of epitaxial SiNWs on a Si(111) substrate grown for 100 min at a total pressure of 3 mbar. As almost every SiNW is naturally oriented perpendicular to one set of $\{111\}$ planes, the orthographic projection on the substrate form a regular triangular network. The light spots in the plane view image are the SiNWs grown perpendicular to the substrate whereas the other three oblique directions form an angle of about 19.5° with respect to the substrate. The SiNW growth rate was about 33 nm/min and the NWs are typically about 3.3 μm long and slightly tapered, which can be attributed to the uncatalyzed deposition of Si on the sides of wires during growth.³⁹ The TEM image in Figure 1c shows a NW with a diameter of about 100 nm

and dark spots about 7 nm in size on the sidewalls of the NWs. These are supposed to be Au–Si particles formed due to insufficient supply of Si source to the Au–Si eutectic on top of the SiNWs which leads to an enhanced migration of Au atoms on the surface of the NWs.³⁸ The HRTEM micrograph of the crystalline core in Figure 1c shows clearly the Si(111) atomic planes (separation 3.14 Å) perpendicular to the NW axis. The reciprocal lattice peaks, which were obtained from a 2D Fourier transform of the lattice resolved image (inset in Figure 1c), proves that the growth axes are $\langle 111 \rangle$ and for which wires vertical $\{112\}$ facets have been found.⁴⁰ The NWs are usually free of dislocations and stacking faults and are covered by a very thin amorphous oxide layer.

Figure 2a shows the top view SEM image of a sample processed at 15 mbar for 60 min under otherwise identical processing conditions. The higher total pressure and thereby increased SiH_4 pressure results in a larger supply of the Si source. Since, under our growth conditions, the growth rate is limited by the supply of the Si source, the larger supply of Si results in a higher growth rate of roughly 250 nm/min, more than 7 times greater than that at 3 mbar (33 nm/min). A comparison of the NWs in Figure 1b and Figure 2b shows that SiNWs grown at higher rates at the total pressure of 15 mbar show much fewer kinks than those grown at lower rates

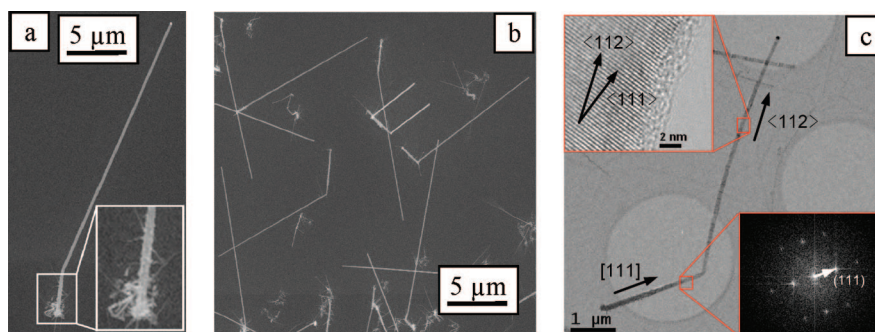


Figure 3. (a) Top view SEM images of a single SiNW grown by dynamically changing the system pressure i.e., first grown at 3 mbar for 70 min and then at 15 mbar for further 30 min. (b) Ensemble of NWs grown by dynamically changing the pressure during the growth. As epitaxy is obtained after the change of the pressure some of the NWs grown in $\langle 112 \rangle$ direction atop of the backbone SiNWs grown in $\langle 111 \rangle$ direction appear parallel in the top view SEM image. (c) Low-magnification TEM image of the SiNW grown in the two step process. The HRTEM image in the inset shows the $\{111\}$ planes near to the $\langle 112 \rangle$ growth direction of the upper part of the SiNW grown at 15 mbar total pressure. FFT of the TEM image confirming the $[111]$ growth direction of the lower part of the SiNW.

under deficient Si supply. The dispersion of the diameters becomes significantly narrower with an average diameter of about 80 nm. The increased silane pressure appears to selectively enhance the catalytic growth process since no tapering due to uncatalytical decomposition of the precursor gas was seen anymore.

The orthographic projection on the Si(111) substrate shows again a triangular network but no NWs growing perpendicular to the substrate surface. Because of the higher supersaturation, epitaxy is less pronounced but, as can be seen clearly in the cross-sectional view in Figure 2b, most of the NWs form an angle of about 70° with respect to the Si(111) substrate indicating a $\langle 112 \rangle$ growth direction. The TEM image in Figure 2c shows the NW to consist of a crystalline core of about 80 nm with no obvious Au–Si particles on the sidewalls. The HRTEM micrograph shows a closer view on the area marked with the red rectangle in the TEM image with the $\{220\}$ atomic planes of the SiNW separated by 0.192 nm, consistent with the tabulated value (0.1919 nm). The $[112]$ growth direction of the SiNW is further confirmed by the HRTEM analysis of the lattice image in $[11\bar{1}]$ projection and its fast Fourier transform (FFT) diffraction pattern with (202), (2 $\bar{2}$ 0), ($\bar{2}$ 20) ($d = 0.192$ nm) and even the (224) lattice planes ($d = 0.111$ nm) well resolved. The $[112]$ nanowire axis in the image is clearly parallel to the FFT of the (224) spot in the diffraction pattern.

It becomes apparent that a transition between the $\langle 111 \rangle$ and the $\langle 112 \rangle$ orientation takes place when changing the total pressure from 3 to 15 mbar. For growth pressures between 3 and 15 mbar, we found a mixed distribution of growth directions.

The pressure-dependence of the growth direction can be demonstrated by changing the pressure dynamically during the growth of SiNWs. For a better visualization we used Au colloids as catalytic particles to get well separated NWs. We first grew at a total pressure of 3 mbar for 70 min and then the pressure was increased to 15 mbar while the flow rate was fixed, and the SiNWs were continuously grown for further 30 min.

A typical SiNW grown using this procedure with obvious two distinct partitions is shown in the SEM image in Figure

3a. The lower, shorter part, which is assumed to be grown during the first 70 min at a total pressure of 3 mbar exhibit extensive branching. The diameter of these core SiNW is about 95 nm, and those of the branches are about 10 nm. It should be stressed here that the branched SiNWs are not grown in one step as no branches were observed for the growth at 3 mbar (see Figure 1a). These branches are formed after changing the total pressure to 15 mbar and can be explained as follows. Migration of Au atoms on the surface of NWs leads to the formation of Au–Si particles about 7 nm in size on the sidewalls of the NWs.³⁸ These particles cover the surface of the SiNWs during growth at 3 mbar, but remain catalytically inactive due to insufficient supply of Si source (see HRTEM image in Figure 1c). By dynamically changing the pressure to 15 mbar the higher total pressure results in a larger supply of the Si source. It is very plausible that because of the enhanced Si supply these small Au–Si eutectic particles on the sidewalls will also catalyze SiNW growth forming branches on the former grown core NWs.

The upper and much longer part of the SiNW spatially separated by a kink from the branched lower part of the NW is supposed to be grown after changing the pressure to 15 mbar. The kinking can be observed by most of such synthesized NWs as shown in Figure 3b and is considered to be due to a change of the growth direction induced by the sudden change of the total pressure during the growth. Some of the NWs grown at 3 mbar with $\langle 111 \rangle$ growth direction are again unambiguously oriented perpendicular to one set of $\{111\}$ planes. As epitaxy is obtained after the change of the pressure some of the NWs grown in $\langle 112 \rangle$ direction atop of the backbone NWs grown at 3 mbar, appear parallel in the top view SEM image in Figure 3b.

The plan-view TEM image in Figure 3c shows such a typical SiNW achieved by dynamically changing the pressure during the growth. The as grown SiNWs were separated from the substrates by ultrasonication in ethanol, and the solvent containing SiNWs was dropped onto a carbon grid. Structural characterization of a large number of such samples showed that the lower roughly $2.4 \mu\text{m}$ long branched part of the NWs grown at a pressure of 3 mbar are oriented along the $\langle 111 \rangle$

direction versus the $\langle 112 \rangle$ direction for the roughly $5.5 \mu\text{m}$ long upper part of the NWs grown at 15 mbar. The kinking of the NWs is the result of changing the growth direction from $\langle 111 \rangle$ to $\langle 112 \rangle$ without changing the diameter of the NWs. The $\{111\}$ planes near to the $\langle 112 \rangle$ growth direction can be seen in the HRTEM inset as well as the thin amorphous surface layer of about 1.5 nm. An angle of about 19.5° with respect to the $\langle 111 \rangle$ direction confirms the $\langle 112 \rangle$ growth direction of the top part of the NW grown at 15 mbar.

In our studies of SiNWs growth, we observed that an increasing fraction of NWs growing along the $\langle 112 \rangle$ direction with increasing pressure. While $\langle 112 \rangle$ is the dominating growth direction for oxide assisted synthesis,⁴¹ the $\langle 112 \rangle$ growth direction is not typical for larger diameter NWs grown via the VLS mechanism. SiNWs produced by Lieber and co-workers at 440 °C had $\langle 110 \rangle$ growth directions for smaller wires and the $\langle 111 \rangle$ direction preferred for larger diameter NWs.²⁹ The reason for this lies in the fact that a silicon atom precipitating upon the (111) surface during growth produces the largest decrease in Gibbs free energy, because (111) planes of silicon have the largest density of surface atoms when acting as an interface.⁴² When the diameter is very small, the free energy of the side faces must be taken into consideration^{29,30} and $\langle 110 \rangle$ growth directions became more favorable. At the higher total pressure and thereby enhanced silane pressure, the catalytic particles swell in size because of the higher supersaturation of silicon in the catalytic Au particle. A higher total pressure should therefore rather stabilize the $\langle 111 \rangle$ growth direction.³¹

However the $\langle 112 \rangle$ growth direction has been observed in SiNWs produced via laser ablation,^{43,44} simple physical evaporation of Si,⁴⁵ and SiO₂-enhanced laser ablation.⁴⁶ For all those cases, the SiNWs were plagued with abundant defects such as microtwins, stacking faults, and grain boundaries. By contrast, HRTEM investigations have shown that our SiNWs grown along a $\langle 112 \rangle$ direction are almost defect-free.

One can assume that there may exist a possibility to define and to stabilize the growth direction by controlling the surface conditions already at the onset of the nucleation. This means that during the NW nucleation event, the surface energies influence the SiNW nucleus structure and the growth direction. The higher supersaturation of the catalytic Au–Si alloy at the higher synthesis pressure may influence the spontaneous formation of single crystal silicon nuclei, but when we changed the pressure dynamically during growth, the $\langle 111 \rangle$ growth direction was already predetermined by the first growth at 3 mbar. In these cases, the VLS growth is believed to be determined by the formation of a single low-free-energy solid–liquid interface that is parallel to a single (111) plane.²⁷

However, many aspects of NW growth are beyond the scope of simple arguments based on near equilibrium growth controlled by surface energies. Korgel et al.³⁴ suggested for Ge NWs that the growth rate is important in determining the growth direction. T. Kawashima et al. showed that there are strong correlations between growth rate, crystallinity, and Au particle formation, all of which are controlled by the

amount of Si supplied to the Au catalyst.³⁸ A.F. Morral et al.⁴⁷ reported the formation of wurtzite type SiNWs with diameter between 20 and 100 nm for growth conditions very similar to ours.

The observed growth along the $\langle 112 \rangle$ direction in the high pressure growth experiment suggests an important role for surface energetics. We believe that these preferences may reflect competing catalyst/SiNW interface and SiNW surface energetics, although additional analysis will be needed to define this point in the future. However, it appears that further optimization of the synthesis parameters will provide selective control over the NW growth direction, which would be very valuable for optical and electronic applications.

In summary, we have demonstrated the controlled growth of SiNWs with different growth orientations, specifically by changing the pressure. We found that at 3 mbar a regime of insufficient Si supply results in a low growth rate of SiNWs growing primarily along $\langle 111 \rangle$. At a total pressure of 15 mbar, NWs grow by a much higher rate along $\langle 112 \rangle$. By dynamically changing the system pressure during the growth process morphological changes of the NW growth directions along their length have been demonstrated.

Acknowledgment. This work is partly funded by the Austrian Science Fund (Project No. 18080-N07) and the Austrian Society for Micro- and Nanoelectronics (GMe) for financial support. Technical Support by USTEM TU-Wien is gratefully acknowledged.

References

- (1) Morales, A. M.; Lieber, C. M. *Science* **1998**, 279, 208.
- (2) Martel, R.; Schmidt, T.; Shea, H. *Appl. Phys. Lett.* **1998**, 73, 2447.
- (3) Cui, Y.; Duan, X.; Hu, J.; Lieber, C. M. *J. Phys. Chem. B* **2000**, 104, 5213.
- (4) Xia, Y.; Yang, P.; Sun, Y.; Wu, Y.; Mayer, B.; Gates, B.; Yin, Y.; Kim, F.; Yan, H.; Lieber, C. M. *Adv. Mater.* **2003**, 15, 353.
- (5) Kim, J.; So, H.; Park, J.; Lieber, C. M. *Appl. Phys. Lett.* **2002**, 80, 3548.
- (6) Gudiksen, M. S.; Lauhon, L. J.; Wang, J.; Smith, D. C.; Lieber, C. M. *Nature* **2002**, 415, 617.
- (7) Martensson, T.; Borgstrom, M.; Seifert, W.; Ohlson, B. J.; Samuelson, L. *Nanotechnology* **2003**, 14, 1255.
- (8) Haraguchi, K.; Katsuyama, T.; Hiruma, K.; Ogawa, K. *Appl. Phys. Lett.* **1992**, 60, 745.
- (9) Duan, X.; Huang, Y.; Cui, Y.; Wang, J.; Lieber, C. M. *Nature* **2001**, 409, 66.
- (10) Wang, J.; Gudiksen, M. S.; Duan, X.; Cui, Y.; Lieber, C. M. *Science* **2001**, 293, 1455.
- (11) Cui, Y.; Lieber, C. M. *Science* **2001**, 291, 851.
- (12) Huang, Y.; Duan, X.; Cu, Y.; Lauhon, L. J.; Kim, K.-H.; Lieber, C. M. *Science* **2001**, 294, 1313.
- (13) Bjork, M. T.; Ohlsson, B. J.; Thelander, C.; Persson, A. I.; Deppert, K.; Wallenberg, L. R.; Samuelson, L. *Appl. Phys. Lett.* **2002**, 81, 4458.
- (14) De Franceschi, S.; van Dam, J. A.; Bakkers, E. P. A. M.; Feiner, L. F.; Gurevich, L.; Kouwenhoven, L. P. *Appl. Phys. Lett.* **2003**, 83, 344.
- (15) Law, M.; Goldberger, J.; Yang, P. *Annu. Rev. Mater. Res.* **2004**, 34, 83.
- (16) Cui, Y.; Wei, Q.; Park, H.; Lieber, C. M. *Science* **2001**, 293, 1289.
- (17) Islam, M. S.; Sharma, S.; Kamins, T. I.; Williams, R. S. *Nanotechnology* **2004**, 15, L5.
- (18) Brus, L. *J. Phys. Chem.* **1994**, 98, 3575.
- (19) Yorikawa, H.; Uchida, H.; Murmatsu, S. *J. Appl. Phys.* **1996**, 79, 3619.
- (20) Mozos, J. L.; Machado, E.; Hernandez, E.; Ordejón, P. *Int. J. Nanotechnol.* **2005**, 2, 114.
- (21) Wagner, R. S.; Ellis, W. C. *Appl. Phys. Lett.* **1964**, 4, 89.
- (22) Arakawa, Y. *Solid-State Electron.* **1994**, 37, 523.
- (23) Tchernycheva, M.; Harmand, J. C.; Patriarche, G.; Travers, L.; Cirilin, G. E. *Nanotechnology* **2006**, 17, 4025.

- (24) Harmanda, J. C.; Tchernycheva, M.; Patriarchea, G.; Traversa, L.; Glasa, F.; Cirlinb, G. *J. Cryst. Growth* **2007**, *301*, 853.
- (25) Martelli, F.; Piccin, M.; Bais, G.; Jabeen, F.; Ambrosini, S.; Rubini, S.; Franciosi, A. *Nanotechnology* **2007**, *18*, 125603.
- (26) Wang, N.; Tang, Y. H.; Zhang, Y. F.; Lee, C. S.; Lee, S. T. *Phys. Rev. B* **1998**, *58*, R16024.
- (27) Wagner, R. S. In *Whisker Technology*; Levitt, A. P., Ed.; Wiley-Interscience: New York, 1970.
- (28) Givargizov, E. I. *J. Cryst. Growth* **1975**, *31*, 20.
- (29) Cui, Y.; Lauhon, L. J.; Gudiksen, M. S.; Wang, J.; Lieber, C. M. *Appl. Phys. Lett.* **2001**, *78*, 2214.
- (30) Wu, Y.; Cui, Y.; Huynh, L.; Barrelet, C. J.; Bell, D. C.; Lieber, C. M. *Nano Lett.* **2004**, *4*, 433.
- (31) Schmidt, V.; Senz, S.; Gösele, U. *Nano Lett.* **2005**, 931.
- (32) Persson, A. I.; Larsson, M. L.; Stenström, S.; Ohlsson, B. J.; Samuelson, L.; Wallenberg, L. R. *Nature* **2004**, *3*, 677.
- (33) Givargizov, E. I.; Sheftal, N. N. *J. Crystal Growth* **1971**, *9*, 326.
- (34) Hanrath, T.; Korgel, B. A. *Small* **2005**, *1*, 717.
- (35) Ozaki, N.; Ohno, Y.; Takeda, S. *Appl. Phys. Lett.* **1998**, *73*, 3700.
- (36) Wu, Y.; Yang, H.; Huang, M.; Messer, B.; Song, J. H.; Yang, P. *Chem.—Eur. J.* **2002**, *8*, 1260.
- (37) Latu-Romain, L.; Mouchet, C.; Cayron, C.; Rouviere, E.; Simonato, J.-P. *J. Nanopart. Res.* DOI 10.1007/s11051-007-9350-3.
- (38) Kawashima, T.; Mizutani, T.; Nakagawa, T.; Torii, H.; Saitoh, T.; Komori, K.; Fujii, M. *Nano Lett.* **2008**, *8* (1), 362.
- (39) Kamins, T. I.; Li, X.; Williams, R. S. *Appl. Phys. Lett.* **2003**, *82*, 263.
- (40) Lugstein, A.; Andrews, A. M.; Steinmair, M.; Hyun, Y. J.; Bertagnolli, E.; Weil, M.; Pongratz, P.; Schramböck, M.; Roch, T.; Strasser, G. *Nanotechnology* **2007**, *18*, 355306.
- (41) Yao, Y.; Li, F.; Lee, S. T. *Chem. Phys. Lett.* **2005**, *406*, 381.
- (42) Ghandhi, S. K. *VLSI Fabrication Principles: Silicon and Gallium Arsenide*, 1st ed; Wiley: New York, 1983; Chapter 1.
- (43) Zhou, G. W.; Zhang, Z.; Bai, Z. G.; Feng, S. Q.; Yu, D. P. *Appl. Phys. Lett.* **1998**, *73*, 677.
- (44) Zhang, Y. F.; Tang, Y. H.; Wang, N.; Yu, D. P.; Lee, C. S.; Bello, I.; Lee, S. T. *Appl. Phys. Lett.* **1998**, *72*, 1835.
- (45) Yu, D. P.; Bai, Z. G.; Ding, Y.; Hang, Q. L.; Zhang, H. Z.; Wang, J. J.; Zou, Y. H.; Qian, W.; Xiong, G. C.; Zhou, H. T.; Feng, S. Q. *Appl. Phys. Lett.* **1998**, *72*, 3458.
- (46) Wang, N.; Tang, Y. H.; Zhang, Y. F.; Lee, C. S.; Bello, I.; Lee, S. T. *Chem. Phys. Lett.* **1999**, *299*, 237.
- (47) Morral, A. F.; Arbiol, J.; Prades, J. D.; Cicera, A.; Morante, J. R. *Adv. Mater.* **2007**, *19*, 1347.

NL8011006